Experimental investigation of a linear-chain structure in the nucleus ^{14}C

H. Yamaguchi [a,*], D. Kahl [a,b], S. Hayakawa [a], Y. Sakaguchi [a], K. Abe [a], T. Nakao [a,c], T. Suhara [d], N. Iwasa [e], A. Kim [f,g], D.H. Kim [g], S.M. Cha [f], M.S. Kwag [f], J.H. Lee [f], E.J. Lee [f], K.Y. Chae [f], Y. Wakabayashi [h], N. Imai [a], N. Kitamura [a], P. Lee [i], J.Y. Moon [j,k], K.B. Lee [j], C. Akers [j], H.S. Jung [k], N.N. Duy [l,m], L.H. Khiem [l], C.S. Lee [i]

[a] Center for Nuclear Study (CNS), University of Tokyo, RIKEN campus, 2-1 Hirosawa, Wako, Saitama 351-0198, Japan
[b] School of Physics and Astronomy, the University of Edinburgh, Peter Guthrie Tait Road, Edinburgh EH9 3BF, UK
[c] Advanced Science Research Center, Japan Atomic Energy Agency, Tokai, Ibaraki 319-1195, Japan
[d] Matsue College of Technology, Matsue, Shimane 690-8518, Japan
[e] Department of Physics, Tohoku University, Aoba, Sendai, Miyagi 980-8578, Japan
[f] Department of Physics, Sungkyunkwan University, 2066 Seobu-ro, Jangan-gu, Suwon, Republic of Korea
[g] Department of Physics, Ewha Womans University, Seoul 120-750, Republic of Korea
[h] The Institute of Physical and Chemical Research (RIKEN), 2-1 Hirosawa, Wako, Saitama 351-0198, Japan
[i] Department of Physics, Chung-Ang University, Seoul 156-756, Republic of Korea
[j] Institute for Basic Science, 70, Yuseong-daero 1689-gil, Yuseong-gu, Daejeon 305-811, Republic of Korea
[k] Wako Nuclear Science Center (WNSC), KEK, 2-1 Hirosawa, Wako, Saitama 351-0198, Japan
[l] Institute of Physics, Vietnam Academy of Science and Technology, 10 Dao Tan, Ba Dinh, Ha Noi, Viet Nam
[m] Dong Nai University, Le Quy Don Street, Tan Hiep Ward, Bien Hoa City, Dong Nai, Viet Nam

A R T I C L E   I N F O

A B S T R A C T

It is a well-known fact that a cluster of nucleons can be formed in the interior of an atomic nucleus, and such clusters may occupy molecular-like orbitals, showing characteristics similar to normal molecules consisting of atoms. Chemical molecules having a linear alignment are commonly seen in nature, such as carbon dioxide. A similar linear alignment of the nuclear clusters, referred to as linear-chain cluster state (LCCS), has been studied since the 1950s, however, up to now there is no clear experimental evidence demonstrating the existence of such a state. Recently, it was proposed that an excess of neutrons may offer just such a stabilizing mechanism, revitalizing interest in the nuclear LCCS, specifically with predictions for their emergence in neutron-rich carbon isotopes. Here we present the experimental observation of α-cluster states in the radioactive ^{14}C nucleus. Using the ^{10}Be + α resonant scattering method with a radioactive beam, we observed a series of levels which completely agree with theoretically predicted levels having an explicit linear-chain cluster configuration. We regard this as the first strong indication of the linear-chain clustered nucleus.

Atomic nuclei are frequently observed to manifest effects of a clustered substructure within, and the particular importance of α particle clustering was pointed out even in the earliest works of nuclear physics [1,2]. In 1956, Morinaga [3] came up with the novel idea of a particular cluster state: the linear-chain cluster state (LCCS). In that work, it was suggested that the 7.66-MeV state in ^{12}C –which is now known as the Hoyle state– may correspond to a state of three α particles arranged in a row. Similar α-clustering in other $4n$-nuclei, which are comprised of multiple α particles, was also discussed in the same work. Later, it was shown by Horiuchi [4] that the Hoyle state could be a molecular-like level of ^{8}Be + α, or equivalently three α particles weakly coupled to each other, instead of an LCCS. However, the concept of the LCCS has particularly drawn the attention of nuclear physicists, both experimentally and theoretically. Now the LCCS is commonly considered as extreme and exotic, due to its presumed propensity to exhibit bending configurations. Therefore, its identification would have a strong impact on the research field of quantum many-body systems.

* Corresponding author.
E-mail address: yamag@cns.s.u-tokyo.ac.jp (H. Yamaguchi).

Despite its pursuit by many scientists for more than half a century, up until now the LCCS has been only hypothetical. There have been LCCS candidates, such as the one in ^{16}O proposed by Chevallier et al. [5] based on the large moment of inertia found for an assumed rotational band. However, the spin-parity assignment of the 19.3-MeV level was questioned in later experiments [6,7], and the interpretation as an LCCS was not supported by recent theoretical works [8–10]. As for the carbon isotopes, Itagaki et al. [11] studied α-cluster states in ^{12,14,16}C using a microscopic model. They investigated breathing and bending motions and concluded that ^{16}C might have a linear-chain structure but at high excitation energies $E_{ex} > 20$ MeV. In the work by Oertzen et al. [12], it was proposed that prolate deformed bands should exist in ^{14}C. Their idea was that those bands might be attributed to an underlying LCCS structure, but the reasoning was merely based on the relatively large momentum of inertia, and the spin and parity J^{π} were confirmed only for low-lying levels in the bands. The LCCS in ^{13}C have also been studied both experimentally and theoretically [13–17]; however, there is no agreed-upon interpretation that the observed cluster levels may arise from an LCCS. In summary, there is no clear evidence of any LCCS in nuclei at present.

A theoretical prediction of LCCS in ^{14}C was made by Suhara and En'yo [18] with an antisymmetrized molecular dynamics (AMD) calculation, yielding a prolate band ($J^{\pi} = 0^+, 2^+, 4^+$) that has a configuration of an LCCS at a few MeV or more above the ^{10}Be $+ \alpha$ threshold. They showed that the LCCS is stabilized by its orthogonality to lower-lying states. At lower excitation energy in ^{14}C, there are triaxially deformed cluster states, which are constructed by bases with bending configurations. To fulfill the orthogonality condition between different states, higher-excited LCCSes are prohibited from bending. This is in stark contrast with ^{12}C, where no triaxial bands exist, and therefore such an LCCS-stabilizing mechanism does not work. A further investigation [15] showed that the AMD wavefunction has a configuration in which two α particles and two neutrons are located close to each other, while the remaining α particle is relatively further away, as illustrated in Fig. 1. This implied that such an LCCS could be experimentally accessible from the ^{10}Be $+ \alpha$ channel in a single step. The emergence of the prolate band as LCCSes had been discussed in the previous pioneering work [12], and two essential new features found in [18] are the absence of the negative-parity band, which appears to be contradictory to the concept of the parity inversion doublets [19], and the higher level energies above the ^{10}Be $+ \alpha$ threshold. The former was explained as the result of a stronger mixing of the negative parity LCCS, in which the ^{10}Be core can be rotated easily, with other bending-shaped configurations. The latter can result from the consumption of kinetic energy from the linear-chain alignment.

The excited states in ^{14}C have been studied by various reactions [12,20–27], but only the excitation energies are known for most levels. In the present work we applied the ^{10}Be $+ \alpha$ resonant scattering method in inverse kinematics [28] to identify the predicted LCCS band in ^{14}C. Our experimental setup was similar to the previous one in the ^{7}Be $+ \alpha$ experiment [29], but we placed an extra silicon detector telescope to cover a broader angular range, instead of the NaI detectors, as shown in Fig. 2. The new setup enabled us to perform a reliable analysis on the angular distribution. An advantage of the present method is that only natural parity levels ($\pi = (-1)^J$) are selectively observed since both particles have $J^{\pi} = 0^+$. The coverage of the most forward laboratory angle θ_{lab}, corresponding to the center-of-mass angle $\theta_{c.m.} = 180°$, provided us with the clearest identification of the resonances, because the Coulomb potential scattering is at minimum there, and it suffers the least from the uncertainty of the nuclear phase shift.
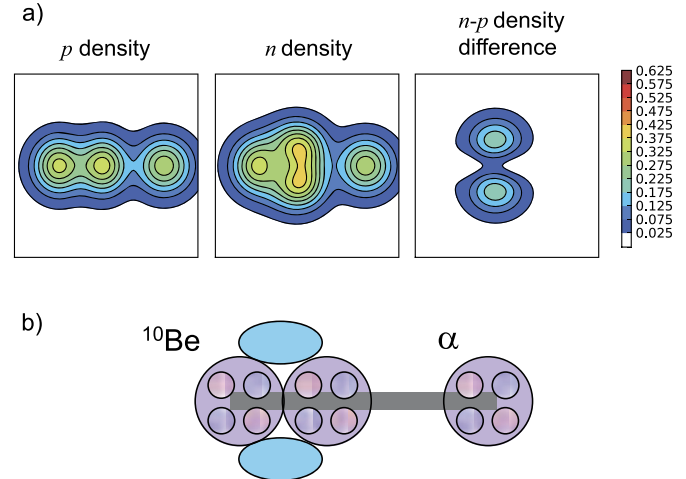

Fig. 1. Wavefunction dominant in the LCCS in ^{14}C calculated by the AMD method [18,15]. a) Proton density ρ_p, neutron density ρ_n and the difference between them. The box size is 10×10 fm^2 for all. b) An intuitive picture of the above wavefunction.
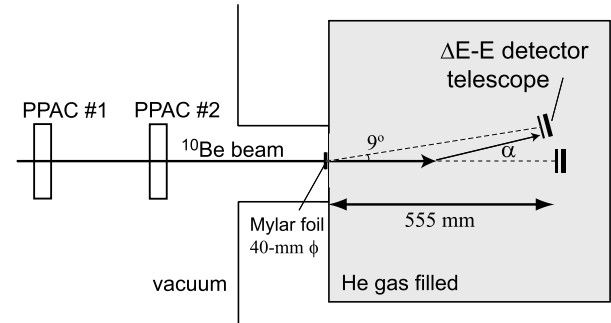

Fig. 2. The experimental setup for the resonant scattering measurement.

Two similar measurements have been independently planned, carried out and published recently. The first work by Freer et al. [30] had a similar setup to ours, but with a more limited angular sensitivity. Another work by Fritsch et al. [31] used an active target setup, but detection was only possible for side scattering angles.

The present measurement was performed at the low-energy radioactive isotope beam separator CRIB [32–34]. The ^{10}Be beam was produced via the ^{11}B(^{2}H, ^{3}He)^{10}Be reaction in inverse kinematics using a 1.2-mg/cm^2-thick deuterium gas target and a ^{11}B beam at 5.0 MeV/u accelerated with an AVF cyclotron. The ^{10}Be beam had a typical intensity of 2×10^4 particles per second, and the beam purity was better than 95%. The beam was counted with two parallel-plate avalanche counters (PPACs), which enabled us to perform an unambiguous event-by-event beam particle identification with the time-of-flight information. The ^{10}Be beam at 25.8 MeV impinged on the gas target, which was a chamber filled with helium gas at 700 Torr (930 mbar) and covered with a 20-μm-thick Mylar film as the beam entrance window. The measured ^{10}Be beam energy at the entrance of the helium gas target, after the Mylar film, was 24.9 ± 0.3 MeV. α particles recoiling to the forward angles were detected by ΔE-E detector telescopes. We used two sets of detector telescopes in the gas-filled chamber, where each telescope consisted of two layers of silicon detectors with the thicknesses of 20 μm and 480 μm. The central telescope was located 555 mm downstream of the beam entrance window exactly on the beam axis, and the other telescope was at an angle of 9° from the beam axis, as viewed from the entrance window position. Each detector in the telescope had an active area of 50×50 mm^2, and 16 strips
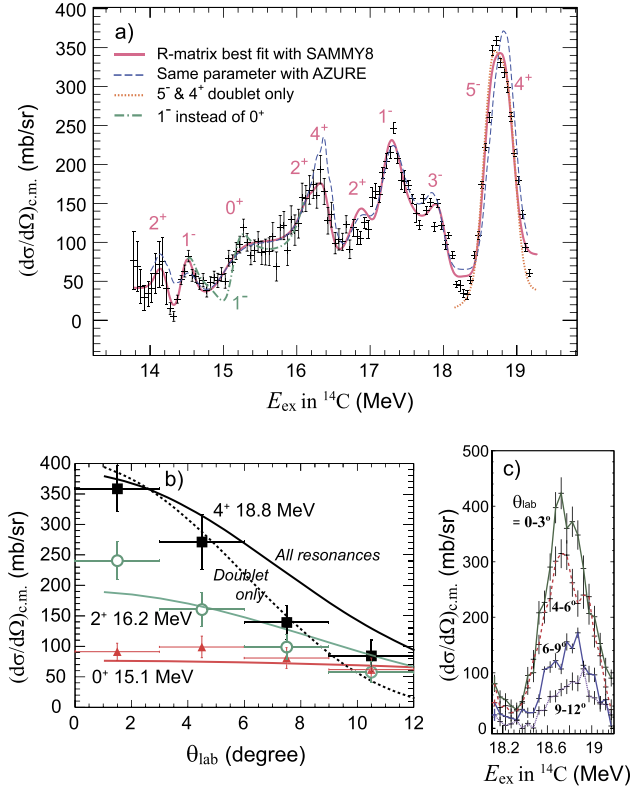
Fig. 3. Experimental center-of-mass cross section of the $^{10}Be + \alpha$ resonant scattering $(d\sigma/d\Omega)_{c.m.}$ a) Excitation function for $\theta_{lab} = 0$–$8°$, fitted with R-matrix calculations; the best R-matrix fit with SAMMY8 [36] (solid curve, $\chi^2/n_{dof} = 62/82$), the same fit but with the 0^+ resonance replaced with 1^- (dash-dotted curve), and another fit only with a doublet of 4^+ and 5^- around 18.7 MeV (dotted curve). The dashed curve is with the above best fit parameters but calculated with AZURE. b) Angular distribution of $(d\sigma/d\Omega)_{c.m.}$ at the resonant energies of the 0^+, 2^+ and 4^+ levels. The present experimental data points are compared with the R-matrix calculations, drawn as the curves. c) Peak profiles around 18.7 MeV for several angular ranges.

for one side, making pixels of 3×3 mm^2 altogether. These detectors were calibrated with α sources, as well as with α beams at various energies produced during the run. The main measurement using the helium-gas target was performed for 2 days, injecting 2.2×10^9 ^{10}Be particles into the gas target as valid events.

We selected genuine scattering events based on the coincidence of a ^{10}Be particle incident on the target, as determined from PPAC trajectory and time-of-flight measurements, with an α particle incident on the silicon detectors. A precise energy loss function of the ^{10}Be beam in the helium gas target was obtained by a direct energy measurement at seven different target pressures interpolated with a calculation using the SRIM [35] code. The scattering position, or equivalently the center-of-mass energy $E_{c.m.}$, was determined by a kinematic reconstruction on an event-by-event basis. The number of events for each small energy division was converted to the differential cross section $(d\sigma/d\Omega)_{c.m.}$, using the solid angle of the detector, the number of beam particles, and the effective target thickness, without any artificial scaling. Finally we obtained the excitation function of the $^{10}Be + \alpha$ resonant elastic scattering for 13.8–19.1 MeV, where events with $\theta_{lab} = 0$–$8°$ ($\theta_{c.m.} = 164$–$180°$) were selected. The overall uncertainty in $E_{c.m.}$ was estimated as 80–110 keV, depending on the energy. The uncertainty mainly originated from the energy straggling of the ^{10}Be and α particles (40–50 keV) and the energy resolution of the detector telescopes (50–100 keV).

The elastic-scattering excitation function we obtained is shown in Fig. 3a. At energies above 15.7 MeV, the excitation function

shows a reasonable agreement in the spectral shape with one of the recent measurements [30], although the previous absolute cross section appears to be larger by a factor of four. We regard the difference as from an error in the overall normalization in the previous work, independent of the energy. In fact, the previous analysis employed a normalization factor to adjust the absolute cross section, while in the present work the cross section was deduced purely from the experimental parameters, which is more reliable. The overall agreement in the spectral shape provides us a confirmation that there is no significant background contribution induced by beam impurities or the inelastic channel, because those depend significantly on the beam and target conditions in the setup, which were quite different between the two measurements. There is a larger disagreement in the lower energy region of 15.0–15.7 MeV, where a correct evaluation of the energy loss function is essential. The peak positions in the present measurement also resemble those of another experiment with a break-up reaction [22]. Finally, the other elastic-scattering measurement [31] yielded smaller cross sections, even much smaller than the Rutherford cross section at low energies. This is fundamental and contradictory to their large Γ_α, but was unexplained. Although they interpret their data as providing clear J^π assignments, their angular distributions show considerable deviation from the calculated distributions, and the separation between the individual resonances was not clearly presented. They claim they identified inelastic scattering events as a sharp locus in the correlation plot of the scattering angles of ^{10}Be and α, but a true inelastic scattering locus will exhibit a variable position depending on $E_{c.m.}$, and the sharp locus never corresponded to the broad $E_{c.m.}$ distribution they observed. Thus we do not employ their results as a credible source in the present discussion.

We performed an R-matrix calculation with SAMMY8 [36] to deduce the resonance parameters. The energy broadening due to the experimental resolution was included in the R-matrix calculation, and the $^{10}Be + \alpha$ channel radius was taken to be 5.0 fm, which was the distance obtained in the AMD calculation. A deviation of ± 0.5 fm in the channel radius was accounted for in the systematic error. We also performed a calculation with AZURE [37] to evaluate the consistency between the calculation codes. We confirmed the results are essentially consistent with one another, although minor differences are seen for closely spaced resonances. The main analysis was performed with a single channel, i.e., only introducing the α particle decay width Γ_α, which is a reasonable assumption to make when considering the basic characteristics of strong α resonances. A multi-channel analysis introducing the $^{13}C + n$ channel was also performed, and the primary effect of the neutron channel was confirmed to be a simple reduction of the resonance height, when the neutron width Γ_n is comparable or larger than Γ_α.

The best fit parameters obtained from the analysis are summarized in Table 1. Also shown in Table 1 are the resonance parameters of the LCCS obtained by the AMD calculation, where the absolute level energies were normalized so that the experimental $^{10}Be + \alpha$ threshold energy at $E_{ex} = 12.01$ MeV is exactly reproduced. Such a normalization is known to provide a better reproducibility of experimental level energies in the vicinity of the threshold, and we adopt the normalized E_{ex} throughout this Letter. Resonances observed in previous experiments with unique determination of J^π are also listed (see [26] for a more complete tabulation, and [30,31] for the latest scattering experiments). We do not find a clear correspondence for most resonances because our measurement selectively observes natural-parity and α-cluster-like states, and is not very sensitive to the high-spin levels close to the $^{10}Be + \alpha$ threshold. Here we describe the identification of the reso-

Table 1

The resonance parameters in ^{14}C determined by the present work, compared with the AMD calculation [18]. Parameters in bold letters are for LCCS predicted in the calculation, and the corresponding experimental resonances. Previously observed states with their J^π determined are also shown, but they do not necessarily correspond to the present measurement. See [12,20–27,30,31] for complete data, including other states. Note that the theoretical E_{ex} is after the threshold normalization.

Present Work				Suhara & En'yo [18]			Other Experiments	
E_{ex} (MeV)	J^π	Γ_α (keV)	θ_α^2	E_{ex} (MeV)	J^π	θ_α^2	E_{ex} (MeV)	J^π
14.21	(2^+)	17(5)	3.5%					
14.50	1^-	45(14)	4.5%				14.67	6^+ [12]
							14.717	4^+ [21]
							14.87	5^- [12]
15.07	**0^+**	**760(250)**	**34(12)%**	**15.1**	**0^+**	**16%**	15.20	4^- [21]
							15.56	3^- [25]
16.22	**2^+**	**190(55)**	**9.1(27)%**	**16.0**	**2^+**	**15%**	15.91	4^+ [21]
16.37	(4^+)	15(4)	3.0%				16.43	6^+ [12]
16.93	(2^+)	270(85)	10.3%				16.9	0^+ [27]
17.25	(1^-)	190(45)	5.5%				17.30	3^- [30]
							17.30	4^- [12]
							17.99	2^+ [30]
18.02	(3^-)	31(19)	1.3%				18.22	4^+ [30]
18.63	5^-	72(48)	9.4%				18.83	5^- [30]
18.87	**4^+**	**45(18)**	**2.4(9)%**	**19.2**	**4^+**	**9%**		

nances around the predicted LCCS energies, which forms the most essential part of the analysis.

1) 15.1 MeV; We observed relatively broad bumps around 14.5 and 15.1 MeV, which are only consistent with low-spin resonances. The best fit for these resonances are with $J^\pi = 1^-$ and 0^+, respectively. If J^π is assigned to be 1^- for the latter, it significantly fails to reproduce the experimental cross sections at the lower energy side of the peak around 15 MeV, as shown as the dash-dotted curve in Fig. 3a. Therefore, we adopt 0^+ as a unique assignment for the resonance around 15.1 MeV. The angular distribution supports the assignment of 0^+ as well; in Fig. 3b, the angular dependence of the experimental and calculated differential cross sections are compared. The curve for 15.1 MeV is almost flat, being consistent with the $J^\pi = 0^+$ assignment.

2) 16.2 MeV; A peak was observed around 16.2 MeV, and its tail on the low energy side was only consistent with a 2^+ resonance, and it cannot be fitted with a resonance with any other J^π. The sharp drop at the high energy side can be reproduced with another higher-spin resonance, and we introduced a 4^+ resonance to obtain the best fit. Once again, the angular distribution in Fig. 3b is consistent with the above assignment, although not in perfect agreement, showing a modest change according to the angle. The disagreement can be attributed to the interference with the nearby 4^+ resonance.

3) 18.7 MeV; Around 18.7 MeV we observed a strong peak that diminishes quickly as θ_{lab} increases, which is a clear indication of a higher spin ($J > 3$) state. The width of the peak is twice as large as the experimental resolution, and we could not obtain a satisfactory fit with only a single resonance, while the angular distribution is closest to that of a 4^+ resonance. We obtained the best fit for this peak as a doublet of 4^+ and 5^-, from all the possible combinations of two resonances. A closer look at the resonance profiles at different angles is given in Fig. 3c, and one may notice that the centroid of the peak is increasing as θ_{lab} is increased. This is consistent with the J^π assignment, in which a lower-spin resonance is located at the higher-energy side. In the previous work [30], the J^π assignment of the resonance was 5^- and they also introduced an additional 4^+ resonance, but at the low-energy side. We could not obtain a perfect fitting for the tails of this strong peak, namely around 18.2 and 19.2 MeV, due to an artifact of the R-matrix calculation induced by the inclusion of low-spin resonances. The dotted curves in Fig. 3a and 3b are formed by fitting only with the doublet, which better reproduces the experimental data.
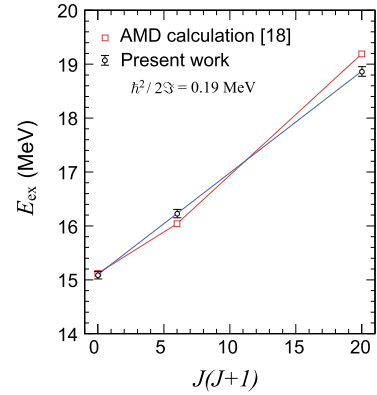
Fig. 4. The $J(J+1)$-dependence of E_{ex} for the band identified in the present experimental work, and the LCCS band predicted in [18].

Although the aforementioned analysis was performed without any assumption from the theoretical calculation, we identified three resonances perfectly corresponded to the predicted LCCS band; J^π are identical, and their energies and spacings are consistent with the theoretical prediction. To illustrate the rotational feature of these levels, the experimental and theoretical level energies are plotted against $J(J+1)$ in Fig. 4. It shows that both sets are almost on the same line, $E_J = E_0 + \hbar^2/2\Im(J(J+1))$, where $\Im$ is the moment of inertia of the nucleus. The linearity allows us to interpret the levels as a rotational band, and the low $\hbar^2/2\Im = 0.19$ MeV implies the nucleus could be strongly deformed, consistent with the interpretation of an LCCS. Although we observed several negative-parity resonances, we could not identify a negative-parity rotational band, which could be expected as the counterpart of the parity inversion doublet. This shows that either the band is out of the sensitivity of our measurement, or the negative-parity LCCSes are dissipated to other states as envisaged by [18].

The experimental Γ_α of these resonances are also compared with the theoretical predictions in terms of the dimensionless partial width θ_α^2 in Table 1, although the precision of both is quite limited. The experimental θ_α^2 was calculated as $\theta_\alpha^2 = \Gamma_\alpha/\Gamma_w$, where Γ_w is the Wigner limit of Γ_α, given by $\Gamma_w = \frac{2\hbar^2}{\mu R^2}P_l$. Here, μ is the reduced mass of the system and P_l is the penetrability of the α particle in the nucleus calculated with the interaction radius

of $R = 5.0$ fm, for a given orbital angular momentum l. It is not straightforward to obtain the theoretical θ_α^2 with an AMD calculation, and in the present work, we calculated θ_α^2 with the method which evaluates the widths using the overlap between the AMD and Brink wavefunctions [38].

The calculation qualitatively reproduces the feature that the experimental θ_α^2 is anti-correlated with J. This behavior corresponds to the reduction in the overlap of the LCCS and the ${}^{10}\text{Be}(0^+) + \alpha$ channel wavefunctions for the higher-spin resonance found in the previous calculation [39], which can be explained with the mixed configuration of the LCCS. The 4^+ state is less mixed with the bending configurations in which the core ${}^{10}\text{Be}$ is rotating, resulting in a smaller overlap with the ${}^{10}\text{Be}(0^+) + \alpha$ channel wavefunctions, while the overlap with the ${}^{10}\text{Be}(2^+) + \alpha$ channel is increased instead. The average of θ_α^2 roughly agrees between the experiment and theory, however, the experimental θ_α^2 shows a larger spread between the resonances. What is causing this discrepancy remains to be answered; whether it is from the experimental resolution or a theoretical ambiguity, or physical properties of the resonance states.

There are factors that are not fully included in the calculation, such as 1) the radial motion of α particle, 2) the rotational motion of ${}^{10}\text{Be}$, and 3) the possible fragmentation of the state, coupling with other configurations. The first factor may explain the larger theoretical θ_α^2 of the 2^+ and 4^+ resonances, while the second factor is more relevant in the 0^+ resonance and the θ_α^2 may be underestimated. It is also possible from the third factor that the θ_α^2 of the 0^+ resonance will be enhanced if the coupling of the ${}^{10}\text{Be} + \alpha$ state with the continuum is correctly included.

From the experimental side, there are possible scenarios in which θ_α^2 can deviate beyond the experimental uncertainty assigned in a standard manner. One possibility is that the mixing ratio of the $(5^-, 4^+)$ doublet was not correctly determined, and the actual 4^+ component is stronger. This is possible because of the limited orthogonality between those two resonances, and we evaluate $\theta_\alpha^2(4^+) = 7\%$ as a maximum limit by this effect. Another possibility is that the 4^+ resonance has a large neutron width Γ_n. In that case, Γ_α can be more than 100 keV ($\theta_\alpha^2(4^+) > 5\%$) when the resonance had a broad Γ_n of over 300 keV. There is no prediction of Γ_n available for this resonance, but some of the neighboring resonances are reported to have Γ_n of a similar order.

In summary, we searched for resonances in ${}^{14}\text{C}$ in the energy range $E_{\text{ex}} = 14$–19 MeV with the resonant elastic scattering method and found several α-cluster-like states, obtaining new spectroscopic information as displayed in Table 1. In spite of many previous measurements with various methods, the knowledge of observed resonances was quite limited, or completely absent. We put a special emphasis on the newly identified 3 resonances which exhibit level energy spacings and J^π that perfectly agree with the prediction of a nuclear-cluster band of LCCS. We claim this as the strongest indication of the LCCS ever found. The comparison of the experimental and theoretical θ_α^2 is also performed in this work, and a rough agreement was observed between them. A finer comparison may lead us to a more profound understanding of the LCCS. As investigated in the theoretical calculation of the ${}^{14}\text{C}$ system, the orthogonality between different quantum mechanical states is considered to play a key role in stabilizing the LCCS. Further studies may reveal whether this mechanism is universal in nuclear systems or particular to ${}^{14}\text{C}$. We also note that other exotic cluster rotational bands beyond our experimental sensitivity may exist in ${}^{14}\text{C}$, such as the one discussed in [12]. As an experimental technology, this achievement can be a milestone for the synthesis of nuclear cluster configurations with more exotic topology, such as triangles and rings [40,41].

References

[1] H.A. Bethe, R.F. Bacher, Rev. Mod. Phys. 8 (1936) 82–229.
[2] L.R. Hafstad, E. Teller, Phys. Rev. 54 (1938) 681–692.
[3] H. Morinaga, Phys. Rev. 101 (1956) 254–258.
[4] H. Horiuchi, Prog. Theor. Phys. 53 (1975) 447–460.
[5] P. Chevallier, F. Scheibling, G. Goldring, I. Plesser, M.W. Sachs, Phys. Rev. 160 (1967) 827–834.
[6] M. Freer, N.M. Clarke, N. Curtis, B.R. Fulton, S.J. Hall, M.J. Leddy, J.S. Pople, G. Tungate, R.P. Ward, P.M. Simmons, W.D.M. Rae, S.P.G. Chappell, S.P. Fox, C.D. Jones, D.L. Watson, G.J. Gyapong, S.M. Singer, W.N. Catford, P.H. Regan, Phys. Rev. C 51 (1995) 1682–1692.
[7] N. Curtis, S. Almaraz-Calderon, A. Aprahamian, N.I. Ashwood, M. Barr, B. Bucher, P. Copp, M. Couder, X. Fang, M. Freer, G. Goldring, F. Jung, S.R. Lesher, W. Lu, J.D. Malcolm, A. Roberts, W.P. Tan, C. Wheldon, V.A. Ziman, Phys. Rev. C 88 (2013) 064309.
[8] S. Ohkubo, Y. Hirabayashi, Phys. Lett. B 684 (2010) 127–131.
[9] T. Ichikawa, J.A. Maruhn, N. Itagaki, S. Ohkubo, Phys. Rev. Lett. 107 (2011) 112501.
[10] T. Suhara, Y. Funaki, B. Zhou, H. Horiuchi, A. Tohsaki, Phys. Rev. Lett. 112 (2014) 062501.
[11] N. Itagaki, S. Okabe, K. Ikeda, I. Tanihata, Phys. Rev. C 64 (2001) 014301.
[12] W. Oertzen, H. Bohlen, M. Milin, T. Kokalova, S. Thummerer, A. Tumino, R. Kalpakchieva, T. Massey, Y. Eisermann, G. Graw, T. Faestermann, R. Hertenberger, H.-F. Wirth, Eur. Phys. J. A 21 (2004) 193–215.
[13] M. Milin, W. von Oertzen, Eur. Phys. J. A 14 (2002) 295–307.
[14] N. Itagaki, W. von Oertzen, S. Okabe, Phys. Rev. C 74 (2006) 067304.
[15] T. Suhara, Y. Kanada-En'yo, Phys. Rev. C 84 (2011) 024328.
[16] T. Yoshida, N. Itagaki, T. Otsuka, Phys. Rev. C 79 (2009) 034308.
[17] T. Yamada, Y. Funaki, Phys. Rev. C 92 (2015) 034326.
[18] T. Suhara, Y. Kanada-En'yo, Phys. Rev. C 82 (2010) 044301.
[19] P.A. Butler, W. Nazarewicz, Rev. Mod. Phys. 68 (1996) 349–421.
[20] F. Ajzenberg-Selove, Nucl. Phys. A 523 (1991) 1.
[21] D.A. Resler, H.D. Knox, P.E. Koehler, R.O. Lane, G.F. Auchampaugh, Phys. Rev. C 39 (1989) 766–782.
[22] N. Soić, M. Freer, L. Donadille, N.M. Clarke, P.J. Leask, W.N. Catford, K.L. Jones, D. Mahboub, B.R. Fulton, B.J. Greenhalgh, D.L. Watson, D.C. Weisser, Phys. Rev. C 68 (2003) 014321.
[23] M. Milin, S. Cherubini, T. Davinson, A.D. Pietro, P. Figuera, D. Miljanić, A. Musumarra, A. Ninane, A. Ostrowski, M. Pellegriti, A. Shotter, N. Soić, C. Spitaleri, M. Zadro, Nucl. Phys. A 730 (3–4) (2004) 285–298.
[24] D. Price, M. Freer, S. Ahmed, N. Ashwood, N. Clarke, N. Curtis, P. McEwan, C. Metelko, B. Novatski, S. Sakuta, N. Soić, D. Stepanov, V. Ziman, Nucl. Phys. A 765 (2006) 263–276.
[25] D.L. Price, M. Freer, N.I. Ashwood, N.M. Clarke, N. Curtis, L. Giot, V. Lima, P.M. Ewan, B. Novatski, N.A. Orr, S. Sakuta, J.A. Scarpaci, D. Stepanov, V. Ziman, Phys. Rev. C 75 (2007) 014305.
[26] P.J. Haigh, N.I. Ashwood, T. Bloxham, N. Curtis, M. Freer, P. McEwan, D. Price, V. Ziman, H.G. Bohlen, T. Kokalova, C. Schulz, R. Torabi, W.V. Oertzen, C. Wheldon, W. Catford, C. Harlin, R. Kalpakchieva, T.N. Massey, Phys. Rev. C 78 (2008) 014319.
[27] F. Cappuzzello, D. Carbone, M. Cavallaro, M. Bondì, C. Agodi, F. Azaiez, A. Bonaccorso, A. Cunsolo, L. Fortunato, A. Foti, S. Franchoo, E. Khan, R. Linares, J. Lubian, J.A. Scarpaci, A. Vitturi, Nat. Commun. 6 (2015) 6743.
[28] K.P. Artemov, O.P. Belyanin, A.L. Vetoshkin, R. Wolskj, M.S. Golovkov, V.Z. Gol'dberg, M. Madeja, V.V. Pankratov, I.N. Serikov, V.A. Timofeev, V.N. Shadrin, J. Szmider, Sov. J. Nucl. Phys. 52 (1990) 408.

[29] H. Yamaguchi, D. Kahl, Y. Wakabayashi, S. Kubono, T. Hashimoto, S. Hayakawa, T. Kawabata, N. Iwasa, T. Teranishi, Y. Kwon, D.N. Binh, L. Khiem, N. Duy, Phys. Rev. C 87 (2013) 034303.

[30] M. Freer, J.D. Malcolm, N.L. Achouri, N.I. Ashwood, D.W. Bardayan, S.M. Brown, W.N. Catford, K.A. Chipps, J. Cizewski, N. Curtis, K.L. Jones, T. Munoz-Britton, S.D. Pain, N. Soić, C. Wheldon, G.L. Wilson, V.A. Ziman, Phys. Rev. C 90 (2014) 054324.

[31] A. Fritsch, S. Beceiro-Novo, D. Suzuki, W. Mittig, J.J. Kolata, T. Ahn, D. Bazin, F.D. Becchetti, B. Bucher, Z. Chajecki, X. Fang, M. Febbraro, A.M. Howard, Y. Kanada-En'yo, W.G. Lynch, A.J. Mitchell, M. Ojaruega, A.M. Rogers, A. Shore, T. Suhara, X.D. Tang, R. Torres-Isea, H. Wang, Phys. Rev. C 93 (2016) 014321.

[32] S. Kubono, Y. Yanagisawa, T. Teranishi, S. Kato, T. Kishida, S. Michimasa, Y. Ohshiro, S. Shimoura, K. Ue, S. Watanabe, N. Yamazaki, Eur. Phys. J. A 13 (2002) 217.

[33] Y. Yanagisawa, S. Kubono, T. Teranishi, K. Ue, S. Michimasa, M. Notani, J.J. He, Y. Ohshiro, S. Shimoura, S. Watanabe, N. Yamazaki, H. Iwasaki, S. Kato, T. Kishida, T. Morikawa, Y. Mizoi, Nucl. Instrum. Methods Phys. Res., Sect. A 539 (2005) 74–83.

[34] H. Yamaguchi, Y. Wakabayashi, G. Amadio, S. Hayakawa, H. Fujikawa, S. Kubono, J. He, A. Kim, D. Binh, Nucl. Instrum. Methods Phys. Res., Sect. A 589 (2008) 150–156.

[35] J. Ziegler, J. Biersack, M. Ziegler, SRIM the Stopping and Range of Ions in Matter, Lulu Press, Morrisville, USA, 2008.

[36] N. Larson, A Code System for Multilevel R-Matrix Fits to Neutron Data Using Bayes' Equations, ORNL/TM-9179/R5, 2000, unpublished.

[37] R.E. Azuma, E. Uberseder, E.C. Simpson, C.R. Brune, H. Costantini, R.J. de Boer, J. Görres, M. Heil, P.J. LeBlanc, C. Ugalde, M. Wiescher, Phys. Rev. C 81 (2010) 045805.

[38] Y. Kanada-En'yo, T. Suhara, Y. Taniguchi, Prog. Theor. Exp. Phys. 2014 (2014) 073D02.

[39] T. Suhara, Y. Kanada-En'yo, ^{10}Be $+ \alpha$ correlation in ^{14}C, in: Hadron and Nuclear Physics, Proceedings, International Workshop, HNP09, Osaka, Japan, November 16–19, 2009, 2010, pp. 366–369.

[40] N. Itagaki, T. Otsuka, K. Ikeda, S. Okabe, Phys. Rev. Lett. 92 (2004) 142501.

[41] D. Wilkinson, Nucl. Phys. A 452 (1986) 296–350.